iScience, Volume *26*

Supplemental information

Beta-coronaviruses exploit cellular stress responses by modulating TFEB and TFE3 activity

Pablo S. Contreras, Pablo J. Tapia, Eutteum Jeong, Sourish Ghosh, Nihal Altan-Bonnet, and Rosa Puertollano

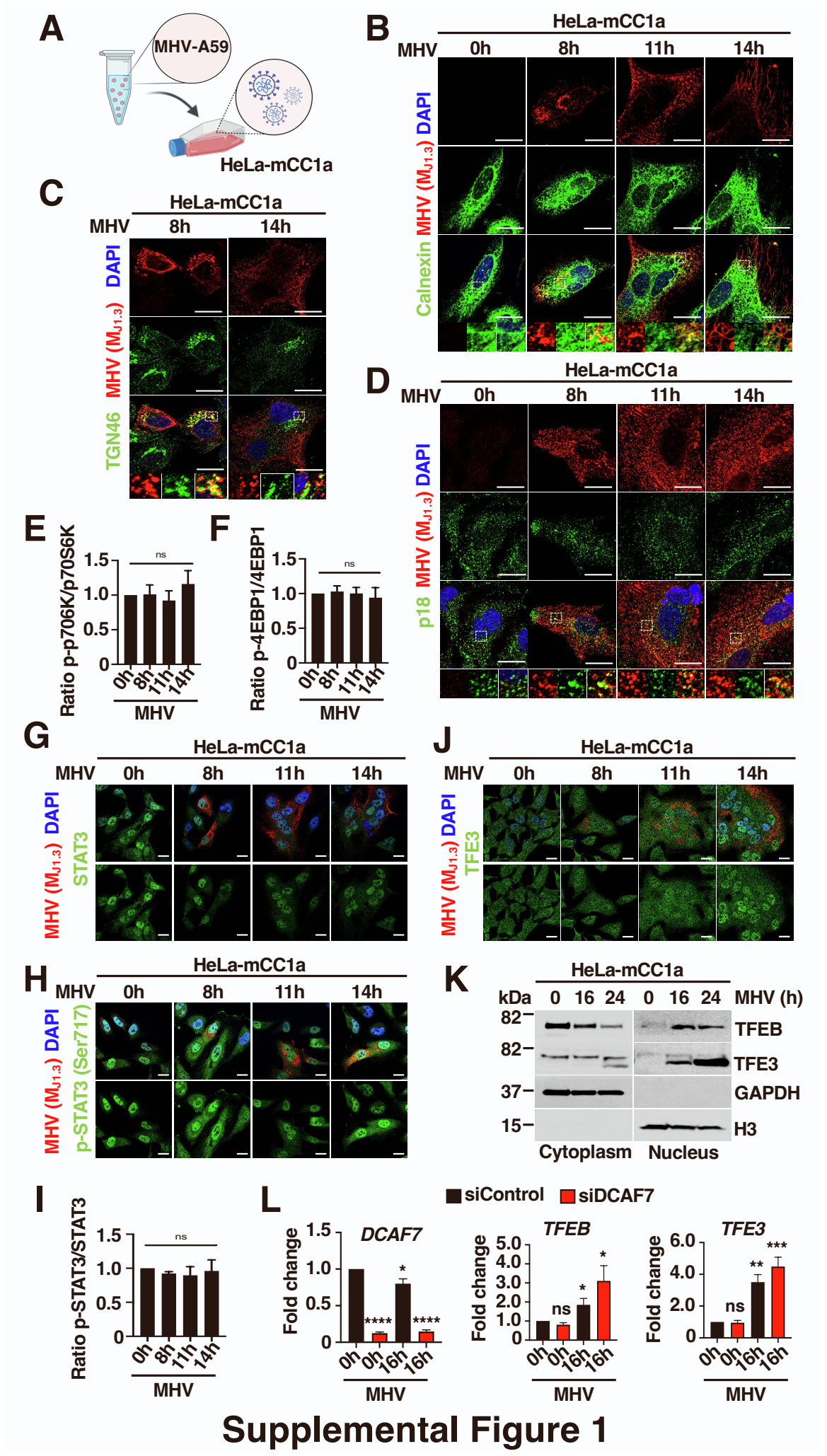

Supplemental Figure 1

Supplemental Figure 1. Kinetic of MHV infection in HeLa-mCC1a cells, Related to Figure 1.

(A) Representative scheme of the experimental system used in this study.

(B) Representative immunofluorescence images of MHV ($M_{j1.3}$) (red) and the ER marker Calnexin (Green) in cells infected with MHV for the indicated times. Cells were stained with DAPI (blue). *n* = 3 independent experiments. Scale bars, 20 μm.

(C) Representative immunofluorescence images of MHV ($M_{j1.3}$) (red) and the TGN marker TGN46 (green) in HeLa-mCC1a cells treated with MHV for 8 h and 14 h. Cells were stained with DAPI (blue). *n* = 3 independent experiments. Scale bars, 20 μm.

(D) Representative immunofluorescence images of MHV ($M_{j1.3}$) (red) and the lysosomal marker p18 (green) in cells infected with MHV for the indicated times. Cells were stained with DAPI (blue). *n* = 3 independent experiments. Scale bars, 20 μm.

(E,F) Quantification of immunoblot data shown in Figure 1A. *n* = 3 independent experiments.

(G) Representative immunofluorescence images of MHV ($M_{j1.3}$) (red) and STAT3 (green) in cells infected with MHV for the indicated times. Cells were stained with DAPI (blue). Scale bars, 20 μm.

(H) Representative immunofluorescence images of MHV ($M_{j1.3}$) (red) and p-STAT3 (Ser717) (green). Cells were stained with DAPI (blue). Scale bars, 20 μm.

(I) Quantification of immunoblot data shown in Figure 1A. *n* = 3 independent experiments.

(J) Representative immunofluorescence images of MHV ($M_{j1.3}$) (red) and TFE3 (green). Cells were stained with DAPI (blue). Scale bars, 20 μM. *n* = 3 independent experiments.

(K) Representative western blot of endogenous TFEB and TFE3 in nuclear/cytoplasmic fractionations of HeLa-mCC1a cells treated with DMSO (0 h) or infected with MHV for 16 h and 24 h. $n = 3$ independent experiments.

(L) Relative quantitative RT-PCR analysis of the mRNA levels of *DCAF7*, *TFEB*, and *TFE3* in cells treated with either siControl or siDCAF7 siRNAs for 72 h followed by infection with MHV for 16 h. $n = 3$ independent experiments.

Statistical analysis with one-way ANOVA followed by Dunnett's multiple comparison post-test. *$p < 0.05$, **$p < 0.01$, ***$p < 0.001$, ****$p < 0.0001$. Data represent mean ± SEM.

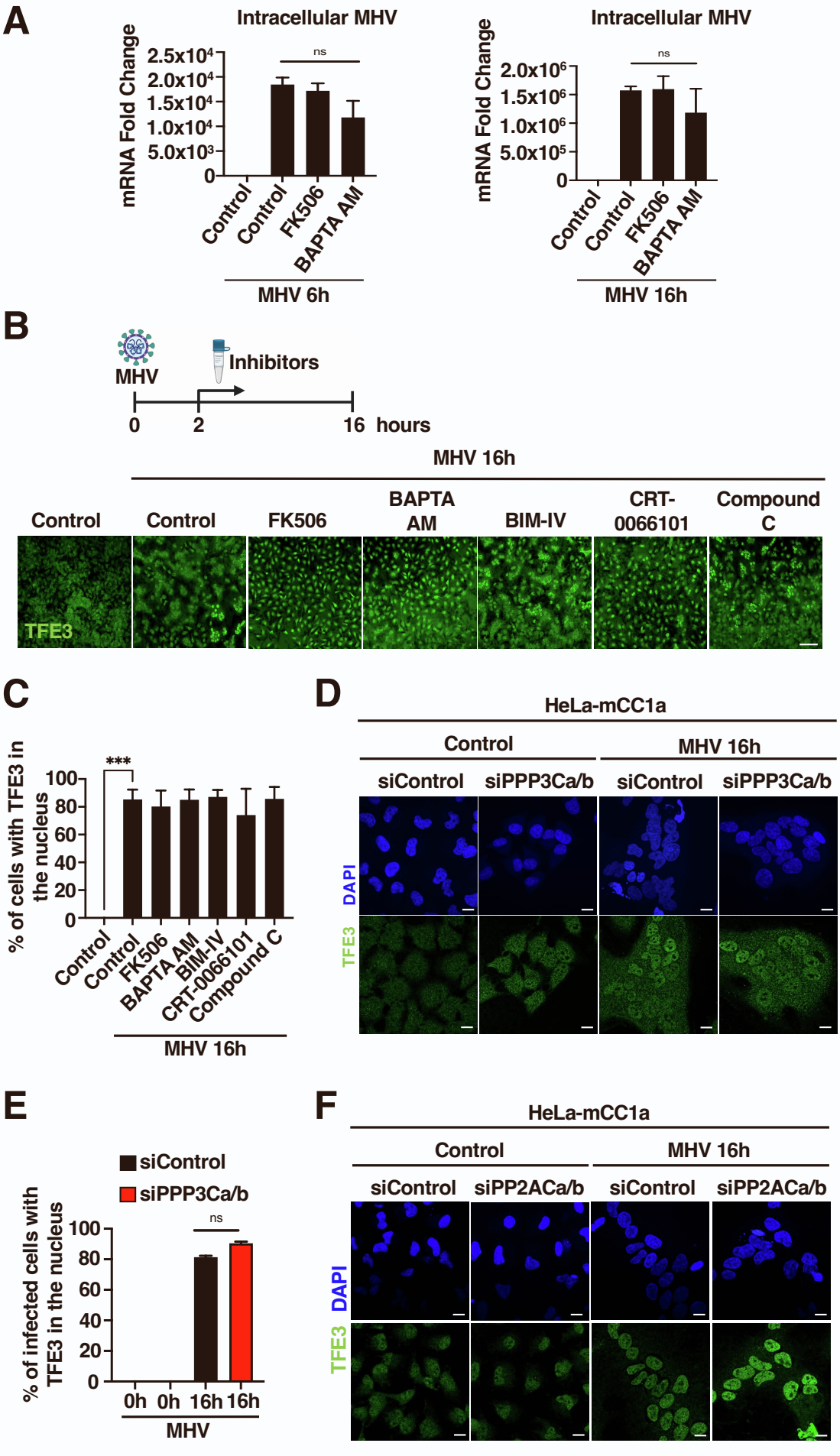

Supplemental Figure 2

Supplemental Figure 2. Calcineurin is not required for MHV-induced TFE3 activation, Related to Figure 2.

(A) Relative quantitative RT-PCR analysis of the MHV M protein mRNA levels in HeLa-mCC1a cells treated with FK506 or BAPTA-AM. *n* = 3 independent experiments.

(B) Representative images of the endogenous TFE3 translocation assay obtained by confocal automated microscopy. HeLa-mCC1a cells were treated with MHV for 16 h. After 2 h of MHV infection, cells were treated with FK506 (calcineurin inhibitor, 10 μM), BAPTA-AM (Ca^{2+} chelator, 10 μM), BIM IV (PKC inhibitor, 1 μm), CRT-0066101 (PKD inhibitor, 2.5 μM), and compound C (AMPK inhibitor, 2.5 μM). *n* = 3 independent experiments. Scale bars, 50 μm

(C) Quantification of average intensity of nuclear endogenous TFE3 fluorescence. Automated imaging analysis included at least 10,000 cells per condition. *n* = 3 independent experiments.

(D) Representative immunofluorescence images of endogenous TFE3 (green) in HeLa-mCC1a cells treated with either non-target or PPP3/calcineurin catalytic subunits A and B siRNAs for 72 h followed by infection with MHV for 16 h. Cells were stained with DAPI (blue) *n* = 3 independent experiments. Scale bars, 20 μm.

(E) Quantification of percentage of infected cells with nuclear TFE3 using confocal microscopy from (D). n = 600 cells per condition from 3 independent experiments.

(F) Representative immunofluorescence images of endogenous TFE3 (green) in HeLa-mCC1a cells treated with DMSO (Control) or MHV for 16 h and pre-treated with a siRNA against PP2A for 72 h. Cells were stained with DAPI (blue) *n* = 3 independent experiments. Scale bars, 20 μm. Statistical analysis with one-way ANOVA followed by Dunnett's multiple comparison post-test. *p < 0.05, **p < 0.01, ***p < 0.001, ****p < 0.0001. Data represent mean ± SEM.

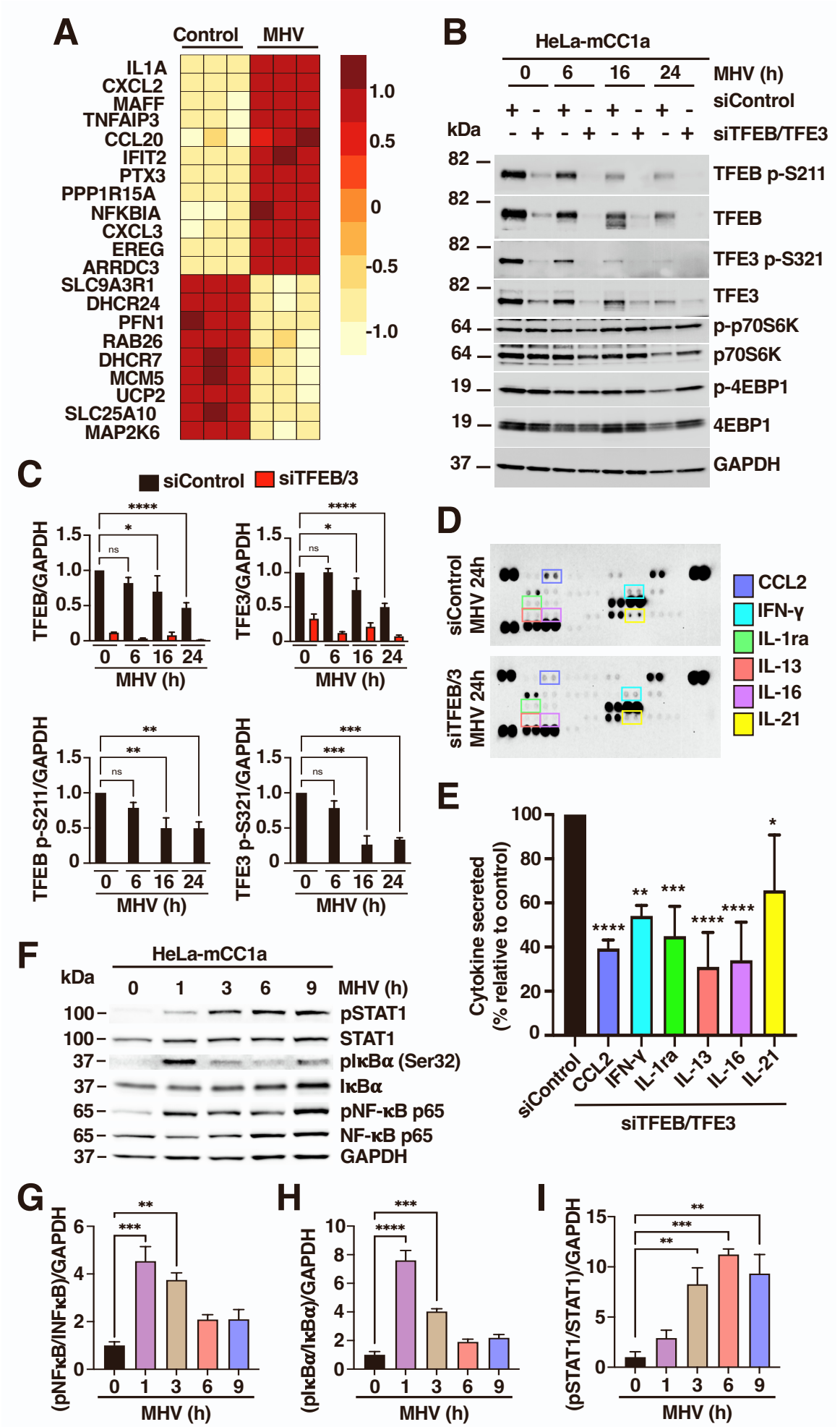

Supplemental Figure 3

Supplemental Figure 3. Cytokine levels are significantly reduced in TFEB/TFE3-depleted cells in response to virus infection, Related to Figure 3.

(A) Heat-map of SARS-CoV-2 infection signature genes in non-infected (Control) versus MHV-infected cells.

(B) Immunoblot analysis of protein lysates from HeLa-mCC1a treated with either non-target or TFEB/TFE3 siRNAs for 72 h followed by infection with MHV at different times. *n* = 3 independent experiments.

(C) Quantification of immunoblot data shown in (B). *n* = 3 independent experiments.

(D) Human cytokine array for siControl and siTFEB/3 cells infected with MHV for 24 h.

(E) Quantification of the percentage of cytokine secretion relative to the control from (D). *n* = 3 independent experiments.

(F) Immunoblot analysis of protein lysates from HeLa-mCC1a cells treated with DMSO (0 h) or infected with MHV for 1 h, 3 h, 6 h, and 9 h. Immunoblots are representative of at least three independent experiments.

(G-I) Quantification of immunoblot data shown in (F). *n* = 3 independent experiments.

Statistical analysis with one-way ANOVA followed by Dunnett's multiple comparison post-test. *p < 0.05, **p < 0.01, ***p < 0.001, ****p < 0.0001. Data represent mean ± SEM.

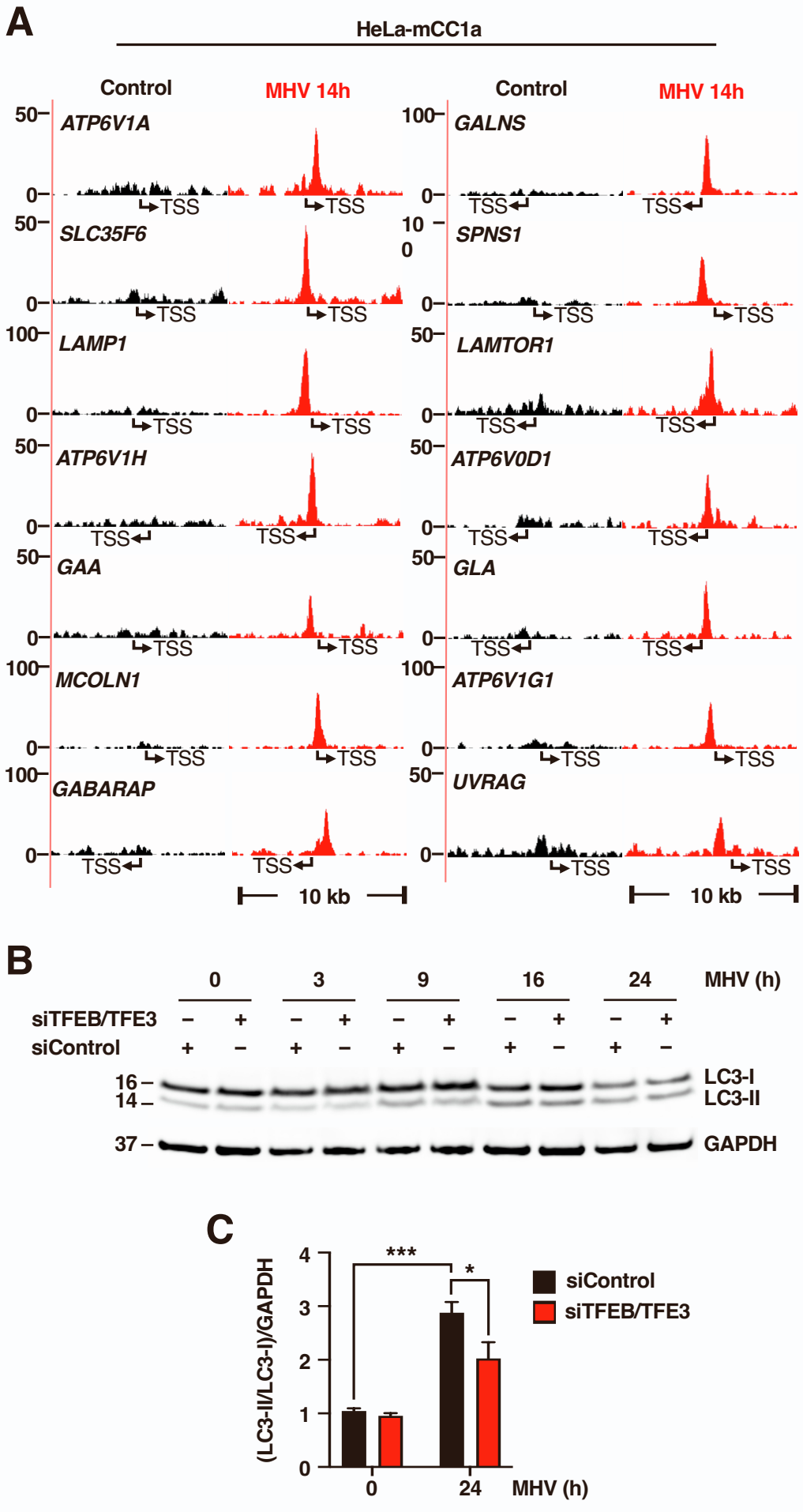

Supplemental Figure 4

Supplemental Figure 4. Chip-seq analysis of TFE3 promoter occupancy for lysosomal genes. Related to Figure 4.

(A) HeLa-mCC1a cells were treated with DMSO (Control) or MHV for 14 h and Chip-seq analysis for endogenous TFE3 was performed. Schematic representations of the TFE3 binding region in the promoter of several lysosome and autophagy genes is shown. The transcription start site is indicated as TSS.

(B) Representative western blot of $LC3_I$ and $LC3_{II}$ levels in HeLa-mCC1a cells treated with either non-target or TFEB/TFE3 siRNAs for 72 h followed by infection with MHV for 3 h, 9 h, 12 h, and 24 h. Immunoblots are representative of at least three independent experiments.

(C) Quantification of immunoblot data shown in (B). $n = 3$ independent experiments.

Statistical analysis with one-way ANOVA followed by Dunnett's multiple comparison post-test. *$p < 0.05$, **$p < 0.01$, ***$p < 0.001$, ****$p < 0.0001$. Data represent mean ± SEM.

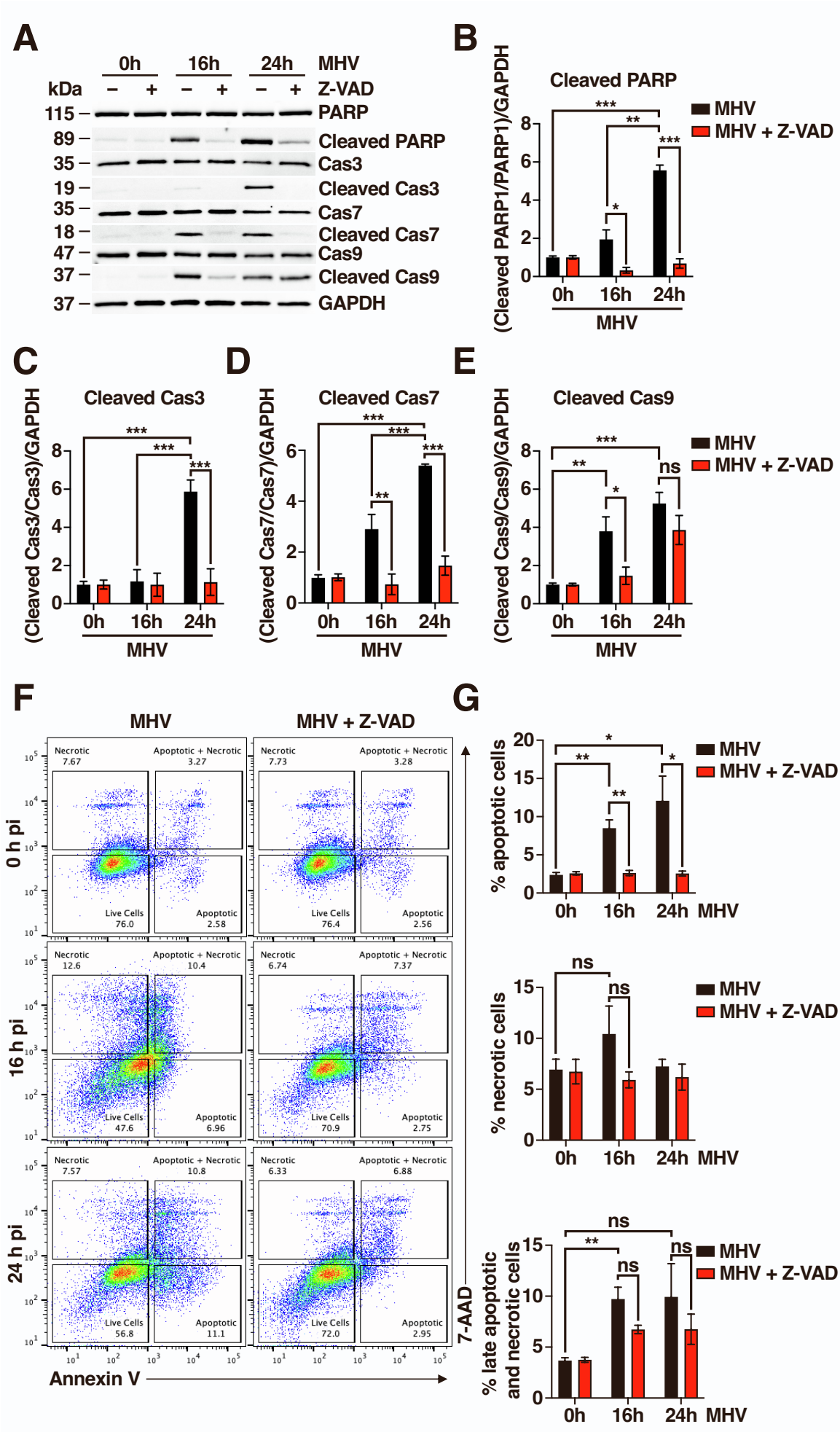

Supplemental Figure 5

Supplemental Figure 5. MHV induces caspase-mediated apoptosis, Related to Figure 5.

(A) Representative western blot of PARP1, Caspase-3, Caspase-7 and Caspase-9 from HeLa-mCC1a cells treated with MHV for 16 and 24 h. After 2 h of infection cells were incubated with a pan-caspase inhibitor Z-VAD (50 μM). *n* = 3 independent experiments.

(B-E) Quantification of immunoblot data shown in (A). *n* = 3 independent experiments.

(F) Representative flow cytometry plots of HeLa-mCC1a cells treated with MHV for 16 h and 24 h. After 2 h of infection cells were incubated with a pan-caspase inhibitor Z-VAD (50 μM). Annexin V+ are apoptotic cells, 7-AAD+ are necrotic cells and Annexin V+/7-AAD+ are late apoptotic and necrotic cells. *n* = 3 independent experiments.

(G) Quantification of the population of apoptotic cells (Annexin V+), necrotic cells (7-AAD+) and late apoptotic and necrotic cells (Annexin+/7-AAD+) from (F). *n* = 3 independent experiments.

Statistical analyzes were performed with Two-way ANOVA with Sıdak's. *$p < 0.05$, **$p < 0.01$, ***$p < 0.001$. Values are mean ± SEM.

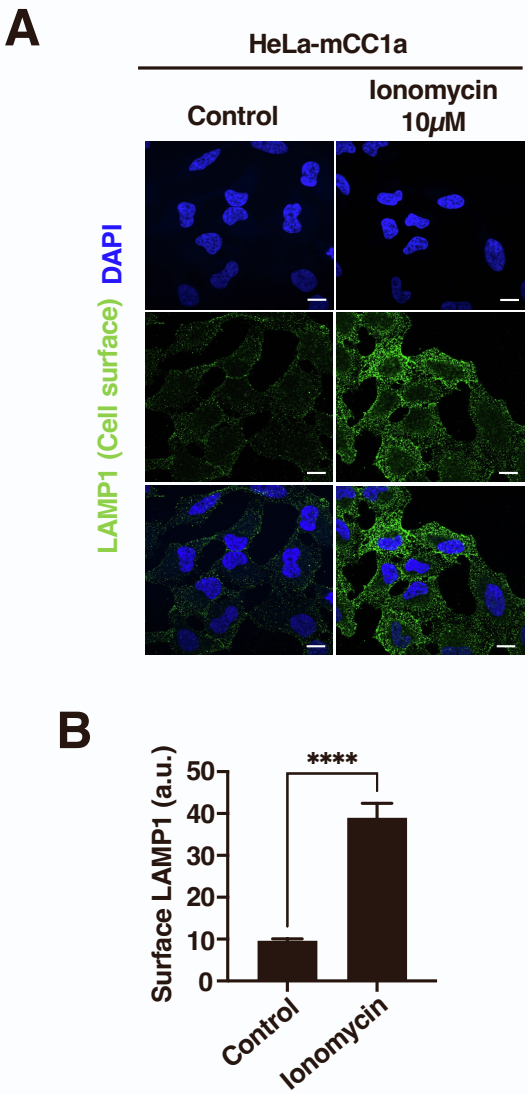

Supplemental Figure 6

Supplemental Figure 6. TFEB and TFE3 depletion decreases viral titer, Related to Figure 6.

(A) HeLa-mCC1a cells were treated with DMSO (control) or Ionomycin (10 μM) for 2 h. Representative immunofluorescence images showing surface LAMP1 levels. *n* = 3 independent experiments. Scale bars, 20 μm.

(B) Quantification of surface LAMP1 levels from (A). n = 30 cells per condition from 3 independent experiments.

(C) Representative plate of crystal violet assay of HeLa-mCC1a incubated with supernatants from MHV-infected siControl or siTFEB/TFE3 cells.

Statistical analysis with Student's t-tests. *$p < 0.05$, **$p < 0.01$, ***$p < 0.001$. Data represent mean ± SEM.

Supplemental Table S3: Top 10 most significant differentially expressed gene sets between control and TFEB/TFE3-depleted cells upon infection with MHV (MSigDB Hallmark 2020), Related to Figure 3.

Term	p-value	q-value	Overlap_Genes
TNFA SIGNALING VIA NFKB	1.45e-54	5.89	[BIRC3, MAP2K3, TNFRSF9, TRAF1, MXD1, KLF6, ATP2B1, PTGS2, FOSL2, NFKB2, EDN1, CXCL2, PPP1R15A, ICAM1, GADD45B, RIPK2, RELB, SERPINE1, SLC16A6, NFKB1, AREG, EHD1, PANX1, BIRC2, SOD2, CD83, VEGFA, HBEGF, BCL6, HES1, IL1A, CCL20, IFIH1, GADD45A, F3, TNFAIP3, SGK1, NR4A3, IFIT2, DUSP1, EGR1, DUSP4, CCRL2, INHBA, PLAU, EGR2]
INFLAMMATORY RESPONSE	1.33e-12	3.04	[TNFRSF1B, ROS1, TNFRSF9, MXD1, GNA15, KLF6, ATP2B1, IL4R, EDN1, ICAM1, OSM, IL2RB, BDKRB1, RIPK2, SERPINE1, AHR, NFKB1, IL10RA, HBEGF, IL1A, CCL20, IL1R1, IL18R1, F3, CCRL2, INHBA, CDKN1A, EREG, IRF1, IL1B, LIF, GCH1, IRAK2, IL6, RNF144B, TLR2, PIK3R5, RGS16, VIP, ADM, FZD5, CYBB, NOD2, BEST1, CXCL11, PTAFR, CXCL8, ADORA2B, HAS2, PTGER4, CHST2, SPHK1, CSF1, HRH1]
IL6 JAK STAT3 SIGNALING	2.23e-05	2.88	[TNFRSF12A, TNFRSF1B, BAK1, IL4R, HMOX1, IL1R1, IL18R1, CNTFR, IRF1, IL1B, IL6, TLR2, INHBE, PIK3R5, CXCL3, CXCL1, CSF2, CXCL11, JUN, CSF1, SOCS3, SOCS1]
P53 PATHWAY	4.88e-11	2.87	[BAK1, MXD1, DNTTIP2, TP63, SESN1, PPP1R15A, HMOX1, CGRRF1, TRIB3, CCP110, FBXW7, CSRNP2, VDR, PRKAB1, HBEGF, IL1A, GADD45A, FOXO3, CDKN1A, BMP2, LIF, SAT1, GLS2, OSGIN1, RGS16, PLK2, NOTCH1, ST14, ATF3, IER5, TGFA, RCHY1, RRAD, CDKN2AIP, FOS, PPM1D, RAD9A, PLK3, DDIT3, BAIAP2, SPHK1, CDK5R1, JUN, AEN, UPP1, SOCS1, TCN2, ZFP36L1, PDGFA, CEBPA, TXNIP]
HYPOXIA	1.54e-09	2.71	[TKTL1, RRAGD, HSPA5, NEDD4L, KLF6, PYGM, RORA, JMJD6, FOSL2, PPP1R15A, HMOX1, PDGFB, SERPINE1, VEGFA, NR3C1, STC2, ERRFI1, F3, TNFAIP3, FOXO3, PGF, DUSP1, SDC4, CDKN1A, AMPD3, ETS1, IL6, PLIN2, ADM, NOCT, ATF3, TIPARP, PHKG1, NFIL3, ANGPTL4, EFNA1, FOS, ADORA2B, PFKFB3, HOXB9, BCL2, ISG20, CHST2, DDIT3, JUN, SIAH2, MAFF, IRS2]

Term	p-value	q-value	Overlap_Genes
IL2 STAT5 SIGNALING	3.42e-09	2.66	[RRAGD, PRKCH, TNFRSF1B, IKZF2, TNFRSF9, TRAF1, MXD1, HIPK2, KLF6, RORA, IL4R, ABCB1, GADD45B, XBP1, IL2RB, CA2, AHR, IL10RA, NOP2, CD83, CISH, IL18R1, SOCS2, TNFRSF8, BMP2, LIF, IRF4, PHLDA1, PTRH2, RGS16, RHOB, PLIN2, FAM126B, TIAM1, EOMES, CSF2, NFIL3, SHE, LRRC8C, BCL2, PUS1, CCR4, DENND5A, CSF1, MAFF, SOCS1, SPRY4]
KRAS SIGNALING UP	1.10e-08	2.59	[BIRC3, TNFRSF1B, FLT4, HDAC9, TRAF1, PTGS2, ABCB1, LAT2, PPP1R15A, CA2, AVL9, DNMBP, CCSER2, IL10RA, CLEC4A, HBEGF, CCL20, IL1RL2, PTBP2, TNFAIP3, ZNF639, INHBA, PLAU, G0S2, EREG, IL1B, BMP2, LIF, ALDH1A2, TPH1, GADD45G, GFPT2, NGF, ETS1, MAP7, SPRY2, DUSP6, RGS16, USP12, PTPRR, HKDC1, CSF2, ANGPTL4, RELN, YRDC, PDCD1LG2]
APOPTOSIS	1.20e-06	2.52	[TNFRSF12A, BIRC3, GNA15, CYLD, GADD45B, HMOX1, DNAJC3, NEDD9, SOD2, IL1A, GADD45A, CTH, CDKN1A, EREG, IRF1, IL1B, BMP2, SAT1, GCH1, IL6, PMAIP1, MCL1, RHOB, SLC20A1, PEA15, ATF3, WEE1, PTK2, ISG20, DDIT3, JUN, EGR3, F2, H1-0, TXNIP, BTG3]
UV RESPONSE UP	5.86e-06	2.43	[BAK1, CXCL2, ABCB1, ICAM1, HMOX1, EIF5, CA2, PPIF, CHKA, SOD2, EPCAM, NR4A1, AGO2, IRF1, FOSB, BMP2, PPAT, GCH1, DNAJB1, IL6, COL2A1, NUP58, CYP1A1, NTRK3, RHOB, HTR7, CEBPG, FGF18, NXF1, ATF3, MSX1, RRAD, FOS, BTG3]
TGF BETA SIGNALING	0.02	2.30	[ARID4B, HIPK2, PPP1R15A, SERPINE1, SMURF2, BMP2, CDK9, BCAR3, SLC20A1, KLF10, TRIM33]

Supplemental Table S4: qPCR primers and siRNA probes, Related to STAR Methods.

REAGENT or RESOURCE	SOURCE	IDENTIFIER
Oligonucleotides		
MHV A59 b Forward CTGACTTGCCCGCTTATGT	IDT	N/A
MHV A59 b Reverse GCTGATTCCTTCTGCCTCTATT	IDT	N/A
ON-TARGETplus Human TFEB siRNA	Horizon Discovery	Cat# L-009798
ON-TARGETplus Human TFE3 siRNA	Horizon Discovery	Cat# L-009363
ON-TARGETplus Human DCAF7 siRNA	Horizon Discovery	Cat# L-019999
ON-TARGETplus Human PPP3CA siRNA	Horizon Discovery	Cat# L-008300
ON-TARGETplus Human PPP3CB siRNA	Horizon Discovery	Cat# L-009704
ON-TARGETplus Human PPP2CA siRNA	Horizon Discovery	Cat# L-003598
ON-TARGETplus Human PPP2CB (5516) siRNA	Horizon Discovery	Cat# L-003599
ON-TARGETplus Non-targeting Control Pool	Horizon Discovery	Cat# D-001810
Hs_ILF3_1_SG QuantiTect Primer Assay	Qiagen	Cat# QT00069524
Hs_GAPDH_2_SG QuantiTect Primer Assay	Qiagen	Cat# QT01192646
Hs_B2M_1_SG QuantiTect Primer Assay	Qiagen	Cat# QT00088935
Hs_SIRT1_1_SG QuantiTect Primer Assay	Qiagen	Cat# QT00051261
Hs_LITAF_1_SG QuantiTect Primer Assay	Qiagen	Cat# QT01013012
Hs_GEM_1_SG QuantiTect Primer Assay	Qiagen	Cat# QT00047964
Hs_IRF9_1_SG QuantiTect Primer Assay	Qiagen	Cat# QT00001113
Hs_FOXO3_1_SG QuantiTect Primer Assay	Qiagen	Cat# QT00031941
Hs_TRIM25_1_SG QuantiTect Primer Assay	Qiagen	Cat# QT01010457
Hs_IL1A_1_SG QuantiTect Primer Assay	Qiagen	Cat# QT00001127
Hs_CXCL8_1_SG QuantiTect Primer Assay	Qiagen	Cat# QT00000322
Hs_CXCL2_1_SG QuantiTect Primer Assay	Qiagen	Cat# QT00013104
Hs_IL24_1_SG QuantiTect Primer Assay	Qiagen	Cat# QT00059059
Hs_PTX3_1_SG QuantiTect Primer Assay	Qiagen	Cat# QT00093261
Hs_TNFAIP3_1_SG QuantiTect Primer Assay	Qiagen	Cat# QT00041853
Hs_RELB_1_SG QuantiTect Primer Assay	Qiagen	Cat# QT00038640
Hs_SH2D5_1_SG QuantiTect Primer Assay	Qiagen	Cat# QT00028525
Hs_CXCL1_1_SG QuantiTect Primer Assay	Qiagen	Cat# QT00199752
Hs_GAPDH_1_SG QuantiTect Primer Assay	Qiagen	Cat# QT00079247
Hs_TFE3_1_SG QuantiTect Primer Assay	Qiagen	Cat# QT00041076
Hs_TFEB_1_SG QuantiTect Primer Assay	Qiagen	Cat# QT00069951
Hs_DCAF7_1_SG QuantiTect Primer Assay	Qiagen	Cat# QT01014300